Neuroscience 549 (2024) 1–12

Contents lists available at ScienceDirect

Neuroscience

journal homepage: www.elsevier.com/locate/nsc

Research Article

Intranasal Administration of Umbilical Cord Mesenchymal Stem Cell Exosomes Alleviates Parkinson's Disease

Weixiao Huang [a], Tao Zhang [a], Xiaodi Li [c], Leilei Gong [b], Yu Zhang [e], Chengcheng Luan [d], Qi Shan [d], Xiaosong Gu [a,b,*], Lili Zhao [b,*]

[a] School of Medicine & Holistic Integrative Medicine, Nanjing University of Chinese Medicine, Nanjing 21000, China
[b] Key Laboratory of Neuroregeneration of Jiangsu and Ministry of Education, Co-innovation Center of Neuroregeneration, Nantong University, Nantong, Jiangsu Province 22600, China
[c] Chinese Medicine Modernization and Big Data Research Center, Nanjing Hospital of Chinese Medicine Affiliated to Nanjing University of Chinese Medicine, Nanjing 21000, China
[d] Academy of Medical Engineering and Translational Medicine, Tianjin University, Tianjin 300000, China
[e] Jiangsu Province Hospital of Chinese Medicine, Nanjing 210000, China

ARTICLE INFO

Key words:
Parkinson's disease
exosomes
olfactory bulb
dopaminergic neurons
inflammation

ABSTRACT

Parkinson's disease (PD) is a common and complex neurodegenerative disease. This disease is typically characterized by the formation of Lewy bodies in multiple brain regions and dopaminergic neuronal loss in the substantia nigra pars compacta, resulting in non-motor symptoms (e.g., olfactory deficits) and motor dysfunction in the late stages. There is yet no effective cure for Parkinson's disease. Considering the neuroprotective effects of exosomes, we investigated whether intranasal administration of umbilical cord mesenchymal stem cell exosomes could improve behavioral functions in PD mice. First, exosomes were endocytosed by the cells *in vitro* and in vivo, indicating that exosomes can cross the blood–brain barrier. Second, we found that both motor and non-motor functions of the PD models were effectively improved during intranasal exosomes treatment. Finally, the activity of olfactory bulb neurons was improved and the loss of dopaminergic neurons in the substantia nigra pars compacta was reversed. Moreover, exosomes attenuated microglia and astrocyte activation, leading to a low level of inflammation in the brain. In conclusion, our study provided a new reference for the clinical application of exosomes in the treatment of PD.

Introduction

Parkinson's disease (PD) is a neurodegenerative disorder. Its main clinical manifestations are motor dysfunctions, including tremor, bradykinesia, rigidity and postural instability (Latif et al., 2021). However, many non-motor symptoms may precede years before motor symptoms (Braak and Del Tredici, 2017). Olfactory impairment is one of the most common and characteristic non-motor features of PD, with a prevalence of 50–90% (Fullard et al., 2017). Currently, Lewy body accumulation and dopaminergic neuronal death in the substantia nigra pars compacta (SNpc) have been identified as the main causes of PD (Tolosa et al., 2021). Therefore, dopamine replacement therapies, such as carbidopa/levodopa or dopamine agonists, are commonly used clinical treatments for PD. These drugs do not save dopaminergic neurons and prevent disease progression, although they do provide some short-term improvement in motor function (Kalia and Lang, 2015). Dopaminergic neuronal death can have various causes, including oxidative stress, neuroinflammation and mitochondrial damage (Jankovic and Tan, 2020). Specific activation of glial cells in the SNpc of mice with PD has been discovered (Hong et al., 2022). Activated glial cells, in turn, secrete cytokines to act on other glial cells or neurons, leading to further accumulation of inflammation and neuronal death (Gao et al., 2022). Therefore, the key to treating PD is to protect dopaminergic neurons and preserve the microenvironment of the SNpc.

Exosomes are extracellular vesicles with a diameter of 40–160 nm, which formed by the multivesicular bodies fusing with plasma membrane (Kalluri and LeBleu, 2020). Exosomes are enriched with a

Abbreviations: EPL, external plexiform layer; GCL, granule cell layer; hUCMSC-Exos, hUCMSCs-derived exosomes; hUCMSCs, Human umbilical cord mesenchymal stem cells; MCL, mitral cell layer; MPTP, 1-methyl-4-phenyl-1,2,3,6-tetrahydropyridine; PD, Parkinson's disease; SNpc, substantia nigra pars compacta.

* Correspondence to: Xiaosong Gu, School of Medicine & Holistic Integrative Medicine, Nanjing University of Chinese Medicine, Nanjing 21000, China.
E-mail addresses: nervegu@ntu.edu.cn (X. Gu), lilizhao22@ntu.edu.cn (L. Zhao).

https://doi.org/10.1016/j.neuroscience.2024.04.010
Received 8 January 2024; Accepted 24 April 2024
Available online 03 May 2024

variety of lipids, proteins, nucleic acids and glycoconjugates (Pegtel and Gould, 2019). Depending on the cells of origin, there are some subtle differences in their contents. Exosomes have a wide range of advantages, including good biocompatibility, low immune response and involvement in cell-to-cell communication (Elsharkasy et al., 2020). Most importantly, exosomes can traverse the blood–brain barrier and therefore have great potential for the treatment of central nervous system disorders. For example, a recent research revealed M2 microglia-derived exosomes can reduce neuronal apoptosis after middle cerebral artery occlusion (Song et al., 2019), bone marrow mesenchymal stem cell-derived exosomes are also neuroprotective for a 3xTg mouse model of Alzheimer's disease (Losurdo et al., 2020). Studies have found that bone marrow mesenchymal stem cell-derived exosomes could rescue dopaminergic neurons and restore motor function in a rat model of 6-hydroxydopamine-induced PD (Mendes-Pinheiro et al., 2019; Cai et al., 2022).

Compared with bone marrow-derived exosomes, umbilical cord mesenchymal stem cell exosomes are enriched with more information on cell cycle, DNA replication and repair (Lei et al., 2021). Therefore, the present study aimed to investigate whether it can improve the functional recovery of the 1-methyl-4-phenyl-1,2,3,6-tetrahydropyridine (MPTP)-induced PD mouse model, as well as the role in neuroprotection and neuroinflammation.

Experimental Procedures

Culture of hUCMSCs

Human umbilical cord mesenchymal stem cells (hUCMSCs) were purchased from Nanjing Tason Biotechnology Co., Ltd. HUCMSCs were cultured with DMEM/F12 (Gibco, Grand Island, USA) containing 10% fetal bovine serum in a cell incubator at 37 ˚C and 5% CO_2. When the cell density reached 80%, the cells were digested with 0.25% trypsin containing EDTA (Gibco) and passaged hUCMSCs at passage 3 were used for subsequent experiments.

Exosome extraction

When the cell density reached 80%, hUCMSCs were cultured in a serum-free medium for 48 h. The supernatant was collected and ultracentrifuged at 400 g for 10 min to remove dead cells and cellular debris, and then filtered through a 0.22 μm filter ((Millipore, Billerica, USA). Exosomes were isolated from 15 mL of cell culture supernatant using the exoEasy Kit (QIAGEN, Hilden, Germany) according to the manufacturer's instruction for specific experimental steps. The filtered supernatant was transferred to a new tube and 1 vol of buffer XBP was added to the supernatant. A total of 30 mL of the mixture was then added to an exoEasy spin column and centrifuged at 500 g for 1 min. After that, 10 mL of buffer XWP was added to the spin column and the residual buffer was removed by centrifugation at 5000 g for 5 min. The spin column was transferred to a new collection tube. Subsequently, 450 μL of buffer XE was added to the membrane and incubated for 1 min. The eluate was collected by centrifugation at 500 g for 5 min and then added to the spin column for further incubation for 1 min. Finally, the eluate was collected by centrifugation at 5000 g for 5 min. The extracted exosomes were resuspended in sterile PBS and stored at −80 ˚C for further use.

Identification and labeling

The morphology of exosomes was observed under a transmission electron microscope. The size of exosomes was measured using nanoparticle tracking analysis (German particle Metrix), and exosome diameters and count were analyzed using ZetaView 8.05.04 (German particle Metrix). Western blot was used to detect the exosome marker CD9, tumor susceptibility gene 101 (TSG101), and the cellular marker Calexin (all from Abcam, Cambridge, UK).

Fluorescent labeling of exosomes was performed according to the instructions of the PKH26 kit (Sigma, St. Louis, USA). Labeled exosomes were added to an Amicon Ultra-15 tube (Millipore, Billerica, USA) and centrifuged at 5000 g for 17 min at 4 ˚C followed by removal of excessive dyestuff. The remaining particles were resuspended in PBS and designated as labeled exosomes.

Olfactory bulb neuron culture and processing

The olfactory bulb was carried out from C57BL/6J mice brain, and then dissected under the microscope with the meninges being peeled off, placed in preheated 0. 25% trypsin (Gibco), cut into 0.5 mm^3, and then cultured at 37℃ for 10–15 min. The digestion reaction of trypsin was terminated with DMEM/F12 containing 10% fetal bovine serum (Gibco). After gently pipetting several times, the prepared cell suspension was centrifuged at 1,200 rpm for 5 min, and the supernatant was discarded. The cell sample was cultured in Neurobasal medium (Gibco) containing 1% glutamine, 2% B27 (Gibco) and 1% PS, passed through a 200 mesh sieve and inoculated onto round coverslips coated with L-polylysine (Sigma). They were placed in an incubator at 37 ˚C, 95% air and 5% carbon dioxide, with the medium changed every 2 days. Subsequent experiments were performed when the neurons grew for 2–3 days.

To detect cellular internalization, labeled exosomes at a concentration of 1×10^{11}/mL were mixed with serum-free DMEM/F12 medium for culturing olfactory bulb neurons, and fixed with 4% paraformaldehyde for 30 min at room temperature after 6, 12, 24, 48 and 72 h of culture. After 1 h of sealing, the sample was incubated with the primary antibody overnight. Nuclei were stained with DAPI and neurons were stained with β-tubulin III (Tuj1, 1:500, Abcam). Internalization of exosomes was detected by a fluorescence microscopy (Zeiss, Oberkochen, Germany).

Mouse PD model preparation and treatment

Male C57BL/6J mice (16 weeks, 25–30 g) were purchased from the Shanghai SLAC Laboratory Animals Co Ltd (Shanghai, China). The animals were housed in SPF conditions with an automatic 12 h/12 h light–dark cycle. Animals were allowed free access to a standard laboratory diet and water. All animal protocols were approved by the Committee of Nantong University and the Administration Committee of Experimental Animals, Jiangsu Province, China (Approval ID: SYXK [SU] 2017–0046).

The PD model was established by intraperitoneal injection of MPTP (Sigma). Prior to the treatment, the mice were trained for 5 days on a pole. For comparability, mice with approximately the same level of locomotor ability were selected to avoid individual differences and divided into control and model groups randomly. The mice in the model group were injected intraperitoneally with MPTP (25 mg/kg/day) for 1 week, and then evaluated behaviorally. Mice in the control group were injected with the same volume of saline. Mice with a significant decrease in the behavioral test compared with control mice were considered to be successfully induced PD model mice for subsequent experiments.

Successful PD model mice were treated with intranasal administration of exosomes (1×10^{11}/mL) or PBS in a volume of 20 μL (10 μL given in the morning and 10 μL given in the evening) every 3 days for 4 times in total. Control mice were given the same volume of PBS. Behavioral and histomorphometric assays were performed at 12, 15, 18 and 21 days of treatment.

For the specific process of exosomes administration, please refer to the patent form (patent application no.CN202210607894.5) submitted by our team.

Endocytosis

After 6 and 48 h of intranasal administration of labeled exosomes, MPTP-treated mice were anesthetized, and their brains were dissociated on dry ice and then embedded in the optimal cutting temperature compound (Tissue-Tek® O.C.T. Compound, Sakura®, Finetek, Torrance, CA, USA). Brain tissue was cut into sections at 10 μm thickness using a slicer (CM1950; Leica, Heerbrugg, Switzerland). The sections were washed thrice with PBS for 3 s, incubated with Alexa Fluor 488-anti-NeuN (1:100, Abcam) at 4 °C for 10 min, washed twice again with PBS and once with DEPC for 3 s, dried for 10 min, and then photographed by the Zeiss fluorescence microscopy.

Behavioral testing

Climbing pole test: we prepared a pole that was 1 cm in diameter and 50 cm in length, with a ball (1.5 cm in diameter) fixed at the top. The pole was placed vertically and the mice were then put onto the ball at the top of the pole. The time for the animal to climb from the top of the pole to the bottom of the pole was recorded, with an interval of 5 min, for 5 records in total. The maximum and minimum values were screened out and averaged.

Buried food-seeking test: Mice were. A clean cage (42 cm long, 24 cm wide, 15 cm high) was prepared and the cheese was embedded in the center, top left, bottom right, top right and bottom left of the clean bedding. The cheese at each site needed to be placed 1 cm below the bedding. The animals, fasted for 24 h beforehand, were gently placed in the center of the cage, and the time for the mice to find the cheese was recorded separately. If the cheese was not found within 300 s, the time was recorded as 300 s. Minimum and maximum values were removed followed by statistical analysis.

Catwalk test: Mice were placed in the behavioral room for 30 min to acclimatize to the dark environment and kept quiet before catwalk testing and behavioral testing. The mice were trained for 5 consecutive days, 5 times per day. On the day of the behavioral test, the trajectory of the mice was recorded as they walked from one end of the catwalk to the other. After testing, movement duration, stride length, and standing time were statistically analyzed.

Tissue acquisition and immunofluorescence

Under deep anesthesia by1.25% Tribromoethanol (Yihe scientific Instrument CO., Ltd, Nanjing, China), mice were perfused by 4% PFA. The brains were then dehydrated via 10%, 20%, and 30% sucrose. The prepared tissue was cryosectioned at a thickness of 12 μm and then performed Immunofluorescence staining. The slices were incubated with the following primary antibodies overnight at 4 °C: GFAP (1:500, Abcam), Iba1 (1:500, Abcam), TH (1:500, Abcam) and pS6 (1:50, Cell Signaling Technology, Danvers, USA). The next day, sections were incubated with cy3-conjugated donkey anti-rabbit antibody (1:500, Sigma), 488-conjugated donkey anti-mouse antibody (1:500, Invitrogen, Carlsbad, USA), and 555-conjugated donkey anti-chicken antibody (1:500, Invitrogen) at room temperature for 1 h. After these steps, the sections were rinsed three times with PBS for 10 min. The samples were visualized under a fluorescence microscopy (Zeiss). Fluorescence intensity was quantified using Image J software (version 1.4.3.67, National Institutes of Health, Bethesda, MD, USA).

Results

Intranasal administration of exosomes improves the behaviors of PD mouse models

We first cultured hUCMSCs *in vitro* and then obtained hUCMSCs-derived exosomes (hUCMSC-Exos) by the *exo*-kit (Fig. 1(**A**)). Under the transmission electron microscopy, the extracted exosomes exhibited a typical double-layer membrane structure with cup-shaped depressions (Fig. 1(**B**)). The result of NTA indicated that the average diameter of these vesicles was 131.8 nm, and the concentration was about 1×10^{11}/mL (Fig. 1(**C**)). In addition, CD9 and Tsg101 as exosome markers were positively expressed in hUCMSC-Exos, and Calexin as cellular markers were expressed in hUCMSCs (Fig. 1(**D**)). Therefore, the hUCMSC-Exos isolated in this study were of high quality and could be used for subsequent experiments.

To investigate the effects of hUCMSC-Exos on PD, we first constructed a classical MPTP-induced PD mouse model. MPTP induces nigrostriatal dopaminergic degeneration leading to motor deficits and non-motor symptoms (olfactory dysfunction), which are fully consistent with the main symptoms of PD in human beings (Langston et al., 1983; Chia et al., 2020). Climbing pole test and buried food-seeking test were performed to detect changes in motor and non-motor functions in mice after MPTP injection and during nasogastric administration of hUCMSC-Exos (Fig. 1(**E**)). Before MPTP intraperitoneal injection, there was no statistically significant difference in the time taken by mice in each group to find the cheese, but after 1 week of MPTP treatment (9d), the time taken to find the cheese in the MPTP group was significantly prolonged, suggesting that the mice had olfactory dysfunction. We assessed the olfactory function of the mice at 12, 15 18, and 21 days following the nasal administration of exosomes. At 12 and 15 days, there was a gradual increase in the time taken to find cheese in the MPTP + PBS and MPTP + Exo groups compared with the control group, suggesting the presence of inertia in the olfactory impairment caused by MPTP. At 18 and 21 days, the time taken to find the cheese in the MPTP + Exo group was drastically shortened, while the time taken to find the cheese in the MPTP + PBS group was also decreased by a very small magnitude, indicating that the olfactory function of the mice would slightly self-recover 2 weeks after MPTP treatment, but the functional recovery was significantly accelerated after the treatment with hUCMSC-Exos (Fig. 1(F)).

Similarly, the time spent on pole climbing was significantly increased in the other groups of mice after MPTP injection compared to the control group. Compared with the MPTP + PBS group, mice in the MPTP + Exo group spent significantly less time climbing poles, indicating that the motor function of PD mice was significantly improved (Fig. 1(**G**)). In addition, the changes in duration, standing time, and stride length of mice in the Catwalk test before and after hUCMSC-Exos treatment were consistent with those in the climbing pole test, but there was no statistical difference (Fig. S1(**A-E**)). Therefore, nasal administration of hUCMSC-Exos could improve both the motor and non-motor functions of PD mice.

Exosomes can be endocytosed by olfactory bulb neurons and dopaminergic neurons

To verify whether the improvements of motor and non-motor functions in mice caused by exosomes, PKH26 was used to label exosomes, and labeled exosomes were then co-cultured with olfactory bulb neurons. Positive signals of PKH26 could be observed in the cytoplasm and neurites from 6 h of co-culture onwards and gradually increased with time (Fig. 2(**A**)). Similar phenomena were observed in olfactory bulb cells cultured *in vitro*, including neurons, astrocytes, microglia, and neural stem cells, suggesting that hUCMSC-Exos can be endocytosed by olfactory bulb cells (Fig. 2(**B**)).

To test whether exosomes could enter the mouse brain by nasal administration, PKH26-labeled exosomes were nasally given to mice. At 6 h after administration, the olfactory bulb and brain of mice were sectioned. We found that there were cytoplasmic aggregates of exosomes in the mitral cell layer (MCL) of the olfactory bulb (Fig. 2(**C**)), and also obvious intracellular aggregates of exosomes in the substantia nigra of the PD model and wildtype mice (Fig. 2(**D**)). Similar exosome endocytosis was also observed in glial cells. After 48 h of nasal

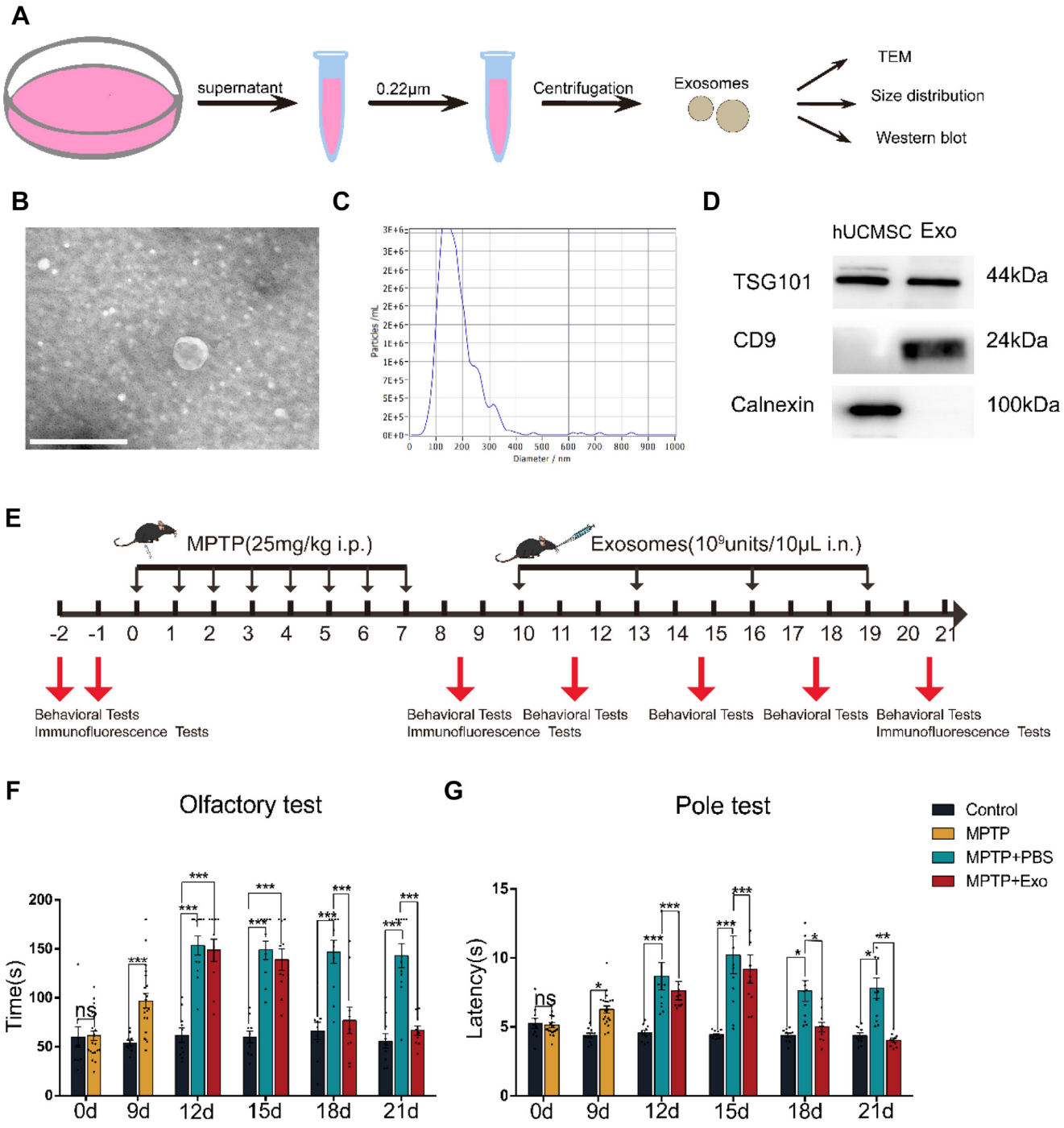

Fig. 1. Human umbilical cord mesenchymal stem cell-derived exosomes (hUCMSC-Exos) ameliorate motor and non-motor deficits in Parkinson's disease (PD) mice. (**A**) Schematic diagram of exosome extraction. (**B**) Representative transmission electron microscopy images of exosomes. Scale bar = 200 nm. (**C**) Size distribution of hUCMSC-Exos measured by nanoparticle tracking analysis. (**D**) Western blot analysis of hUCMSC-Exos markers, including CD9, Tsg101, and Calnexin. (**E**) Schematic diagram of the in vivo experimental protocol. (**F**) Statistics of olfactory test results in mice. The horizontal coordinate is the treatment time, the vertical coordinate is the time spent by a single mouse to find the cheese, and different colors represent different treatments. (**G**) Statistics of the results of the climbing pole test in mice. The horizontal coordinate is the treatment time, the vertical coordinate is the time spent by a single mouse to climb from the top of the pole to the bottom of the pole, and different colors represent different treatments. Data are expressed as mean ± SEM and were analyzed using one-way analysis of variance. $^{*}P < 0.1$, $^{**}P < 0.01$, $^{***}P < 0.001$, ns means no significance.

administration of hUCMSC-Exos, exosomes aggregation was still observed in the olfactory bulb and brain regions of the PD mice, while the signal of exosomes in the wildtype mice gradually decreased over time. (Fig. 2(**C-D**)). These results indicate that exosomes can be endocytosed by cultured olfactory bulb cells, and exosomes can cross the blood–brain barrier to reach the olfactory bulb and substantia nigra at 6 h after intranasal administration, suggesting that exosomes may improve the symptoms of PD after entering the cells.

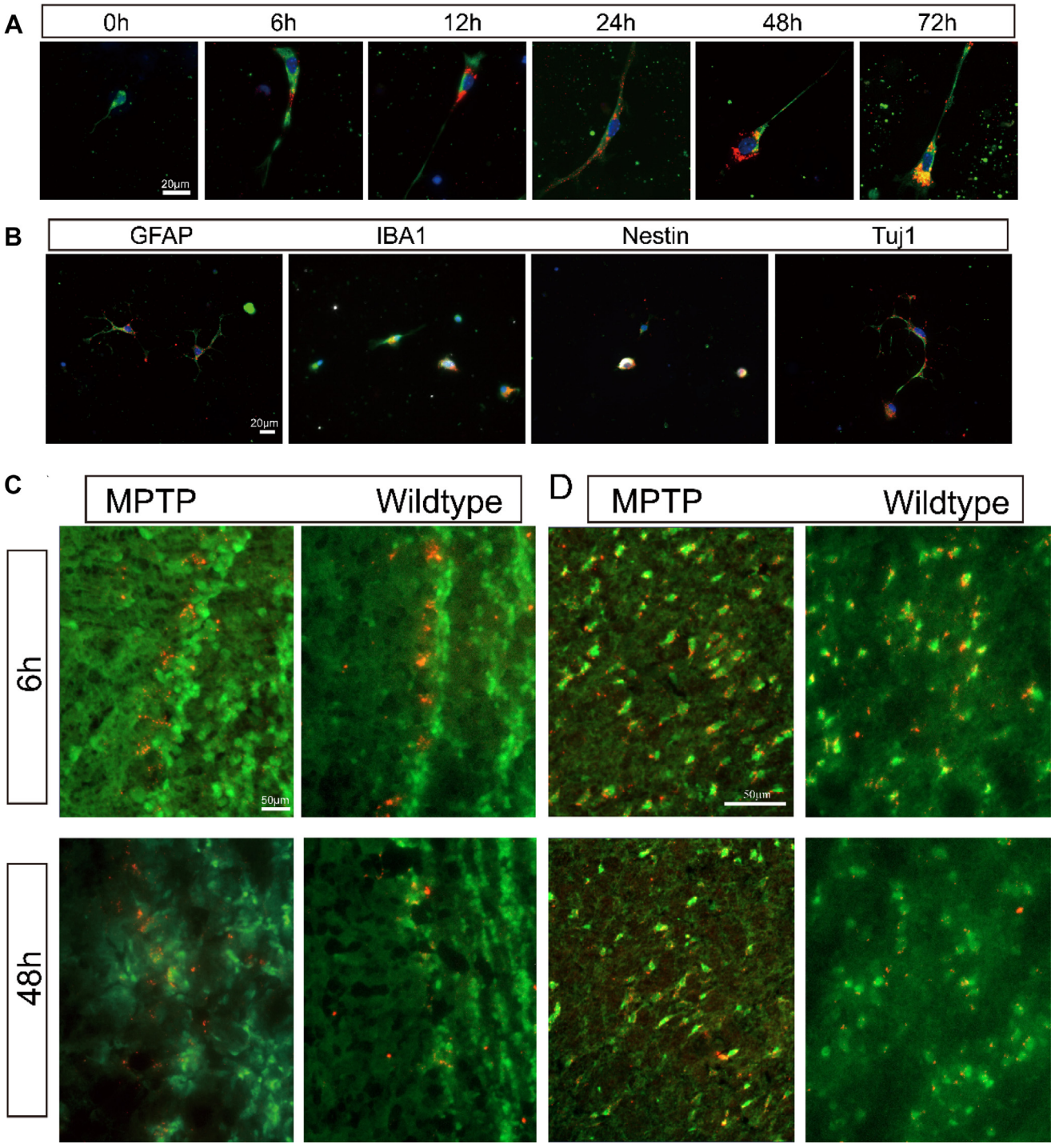

Fig. 2. Accumulation of human umbilical cord mesenchymal stem cell-derived exosomes (hUCMSC-Exos) *in vitro* and in vivo. (**A**) pkh26-labeled hUCMSC-Exos co-cultured with olfactory bulb neurons *in vitro* at different time points. hUCMSC-Exos are labeled by pkh26 (red), Tuj1 (green) indicates olfactory bulb neurons, and nuclei are identified by Hoechst33342 (blue). Scale bar = 20 μm. (**B**) pkh26-labeled hUCMSC-Exos co-cultured with olfactory bulb cells *in vitro* for 24 h. pkh26 (red) labels hUCMSC-Exos, GFAP (green) labels olfactory bulb astrocytes, IBA1 (white) labels microglial cells, and Nestin labels neural stem cells (white) as well as neurons (green), and the nuclei of cells are identified by Hoechst33342 (blue). Scale bar = 20 μm. (**C-D**) Accumulation of pkh26-labeled hUCMSC-Exos in the olfactory bulb and substantia nigra in wildtype and PD mice at 6 and 24 h after intranasal administration. pkh26 (red) labels hUCMSC-Exos, Neun (green) denotes neurons, and the nuclei (blue) are identified by Hoechst. Scale bar = 50 μm. (For interpretation of the references to colour in this figure legend, the reader is referred to the web version of this article.)

Exosome treatment protects the activity of olfactory bulb neurons in PD mouse models

To further verify the effect of nasal exosomes on mouse olfactory bulb neurons, pS6 immunohistochemical analysis was performed to detect the activity of olfactory bulb neurons (LaFever et al., 2022). There were fewer pS6-positive cells in the MCL, external plexiform layer (EPL) and granule cell layer (GCL) of the olfactory bulb in the MPTP group at 9 days (Fig. 3(**A**)). In contrast, pS6 signals were enhanced and the number of pS6-positive cells increased at all layers

of the olfactory bulb at 15, 18 and 21 days after exosome treatment. In comparison, the pS6 signals in the MPTP + PBS group were significantly weaker until day 21, when there was a slight recovery of fluorescence intensity (Fig. 3(**A-D**)). In conclusion, MPTP treatment could cause decreased neuronal activity in the olfactory bulb, whereas exosome treatment could increase the activity of olfactory bulb neurons in mice, suggesting that intranasal administration of hUCMSC-Exos has a neuroprotective effect in olfactory bulb neurons.

Intranasal administration of exosomes alleviates inflammation in the olfactory bulb of PD mouse models

Neuroinflammation is thought to be one of the causes of PD progression and glial cell activation plays a very important role in inflammation. Therefore, the present study also focused on the changes in microglia and astrocytes during intranasal administration of hUCMSC-Exos. IBA1 staining of olfactory bulb sections from mice at

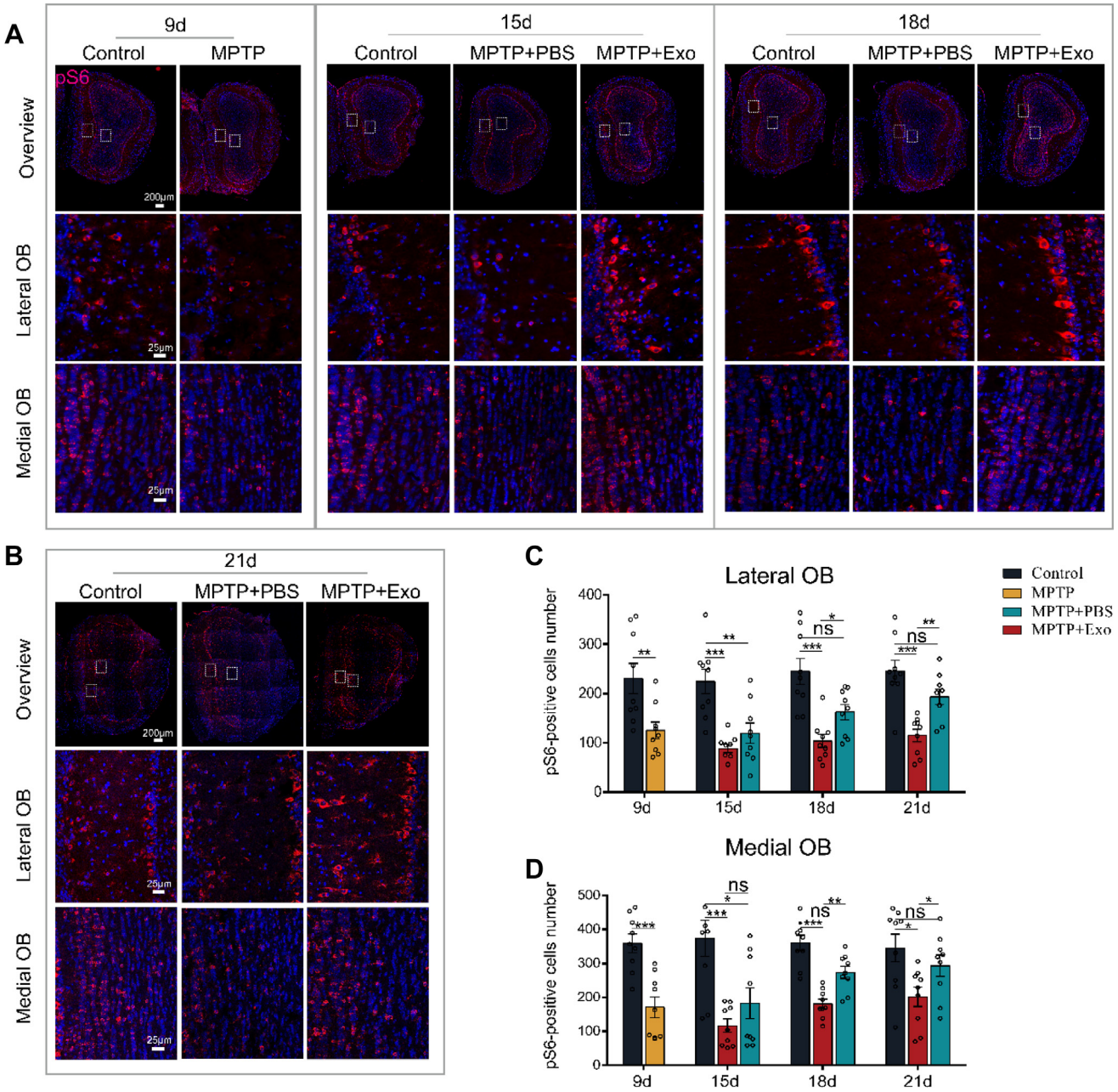

Fig. 3. Changes in olfactory bulb (OB) neuronal activity during intranasal administration of human umbilical cord mesenchymal stem cell-derived exosomes (hUCMSC-Exos). (**A-B**) Coronal sections of the left (Lateral) and middle (Medial) sides of the OB at different treatment time points, with pS6 (red) labeling olfactory bulb neuronal activity and Hoechst33342 (blue) labeling the nuclei. Scale bar = 200 μm, 25 μm. (**C-D**) Lateral OB (C) and Medial OB (D) neuronal activity statistics. The horizontal coordinate is the treatment time, the vertical coordinate is the number of pS6-positive cells, and different colors represent different treatments. $n = 9$, data are expressed as mean ± SEM and were analyzed using one-way analysis of variance. $^{*}P < 0.1$, $^{**}P < 0.01$, $^{***}P < 0.001$, ns means no significance. (For interpretation of the references to colour in this figure legend, the reader is referred to the web version of this article.)

different time points revealed an increased number of IBA1$^+$ microglia, enlarged cell cytosol and shorter processes in the olfactory bulbs of MPTP-injected mice compared with the control group, indicating the activation of microglia (Fig. 4(**A-C**)). Until day 18, microglia in the olfactory bulb of mice in the MPTP + PBS group remained activated (Fig. 4(**A**)). On day 21, the morphology of microglia in the MPTP + PBS group converged to that of the control group (Fig. 4(**A**)). On day 15, the cell body in the MPTP + Exo group became smaller, and some of the processes were thin stripe-shaped (Fig. 4(**A**)). On day 18, the morphology of microglia in the MPTP + Exo group was similar to that of the control group (Fig. 4(**A**)).

In addition, the number of astrocytes immunopositive for GFAP was significantly increased after treatment with MPTP compared with the control group (Fig. 4(**D-F**)). The number of astrocytes started to decrease at around the 15th day after intranasal administration of hUCMSC-Exos, but the number of astrocytes in the PBS group did not decrease significantly and showed the same trend as that of microglia (Fig. 4(**D-F**)). The above results indicate that MPTP treatment leads to the activation of glial cells in the olfactory bulb of PD mouse models, which gradually diminishes over time, whereas intranasal administration of hUCMSC-Exos accelerates the alleviation of inflammation and restores the morphology to the normal situation more quickly.

To explore the origin of activated glial cells, we labeled the mice with EDU on days 15 and 18 when glial cell changes were most pronounced. Surprisingly, co-localization of EDU$^+$ with IBA1$^+$/GFAP$^+$

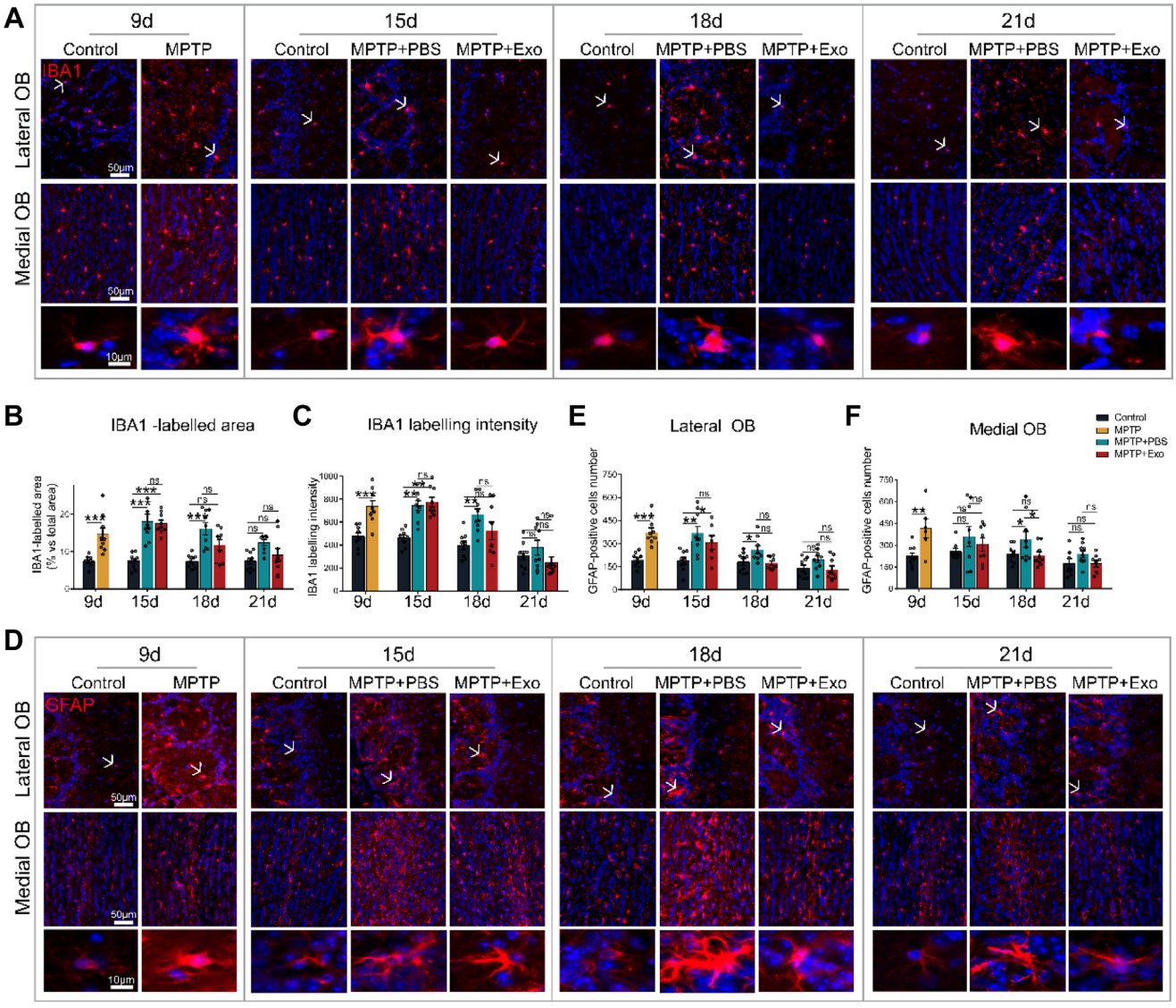

Fig. 4. Changes in microglia and astrocytes in the olfactory bulb (OB) during intranasal administration of human umbilical cord mesenchymal stem cell-derived exosomes (hUCMSC-Exos). (**A**) Coronal sections of the left (Lateral) and middle (Medial) sides of the OB at different treatment time points. IBA1 (red) labels microglia in the OB and Hoechst33342 (blue) labels the nuclei. Scale bar = 50 μm, 10 μm. (**B-C**) The immunolabelling area (B) and intensity (C) of IBA1-positive cells. The horizontal coordinate is the treatment time, the vertical coordinate is the number of IBA1-positive cells, and different colors represent different treatments. $n = 9$, data are expressed as mean ± SEM and were analyzed using one-way analysis of variance. $^*P < 0.1$, $^{**}P < 0.01$, $^{***}P < 0.001$, ns means no significance. (**D**) Coronal sections of the left (Lateral) and middle (Medial) sides of the OB at different treatment time points. GFAP (red) labels astrocytes in the OB and Hoechst33342 (blue) labels the nuclei. Scale bar = 50 μm, 10 μm. (**E-F**) Counts of astrocytes in Lateral OB (E) and Medial OB (F). The horizontal coordinate is the treatment time, the vertical coordinate is the number of GFAP-positive cells, and different colors represent different treatments. $n = 9$, data are expressed as mean ± SEM and were analyzed using one-way analysis of variance. $^*P < 0.1$, $^{**}P < 0.01$, $^{***}P < 0.001$, ns means no significance. (For interpretation of the references to colour in this figure legend, the reader is referred to the web version of this article.)

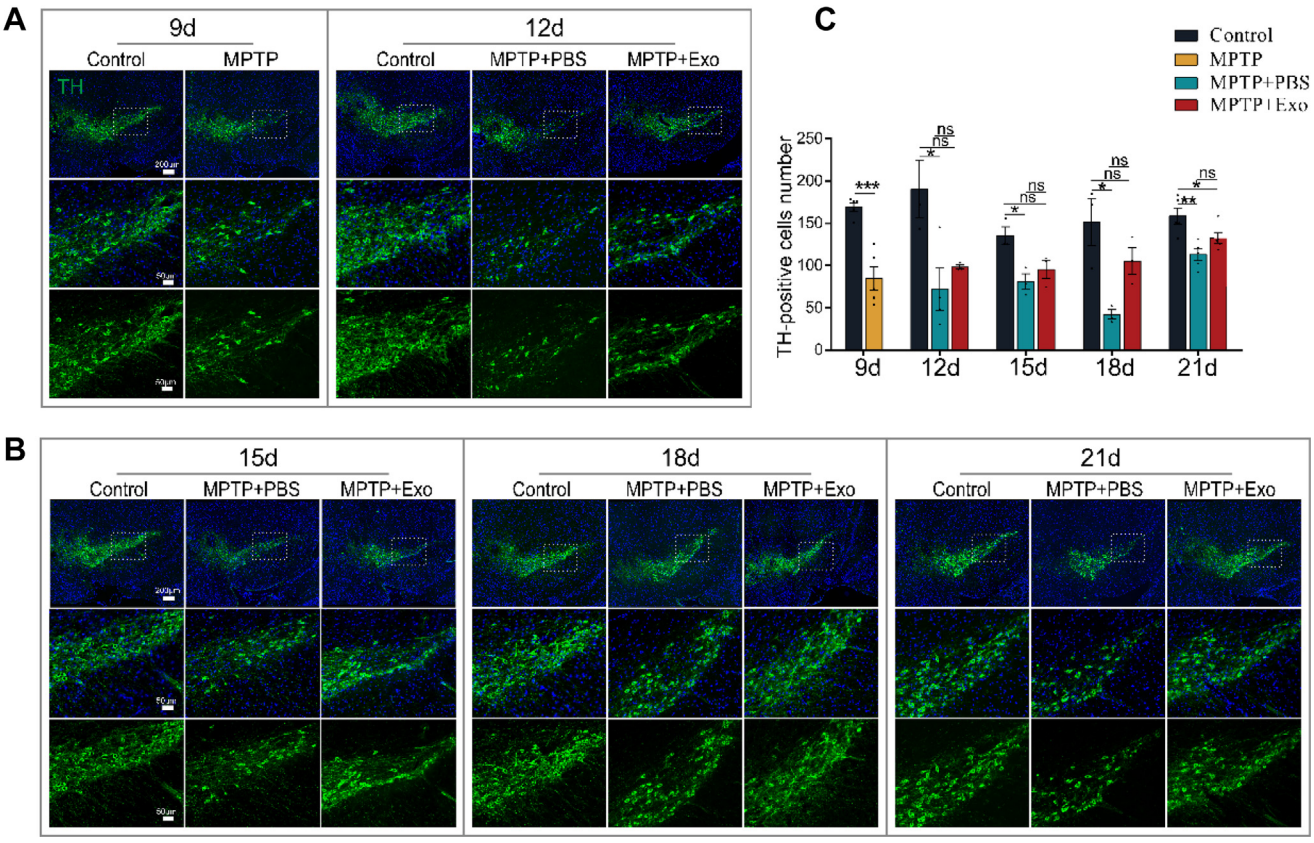

Fig. 5. Changes in dopaminergic neurons in the substantia nigra pars compacta (SNpc) during nasal administration of human umbilical cord mesenchymal stem cell-derived exosomes (hUCMSC-Exos). (**A-B**) Changes in dopaminergic neurons at different treatment time points. Tyrosine hydroxylase (green) labels dopaminergic neurons and Hoechst33342 (blue) labels the nuclei. Scale bar = 200 μm, 50 μm. (**C**) Statistics on the number of dopaminergic neurons in the SNpc. The horizontal coordinate is the treatment time, the vertical coordinate is the number of tyrosine hydroxylase-positive cells, and different colors represent different treatments. $n = 3$, data are expressed as mean ± SEM and were analyzed using one-way analysis of variance. $^{*}P < 0.1$, $^{**}P < 0.01$, $^{***}P < 0.001$, ns means no significance. (For interpretation of the references to colour in this figure legend, the reader is referred to the web version of this article.)

was not observed in all layers of the mouse olfactory bulb, but instead, cell proliferation signals were evident in the middle region of the olfactory bulb, i.e., the subependymal zone and the GCL region. This suggests that activated glial cells may not arise by cell proliferation, but normal glial cells come over through differentiation or migration. In addition, the number of proliferative cells in the MPTP + Exo group was higher than that in the MPTP + PBS group on day 15 (Fig. S2 (**A-C**)), whereas there are reports indicating that neural stem cells are mainly in the subependymal zone (Brill et al., 2009; Porlan et al., 2013). The above results suggest that intranasal administration of hUCMSC-Exos alleviates inflammation in the olfactory bulb of PD mouse models and promotes self-healing of the olfactory bulb.

Intranasal administration of exosomes rescues dopaminergic neurons and attenuates inflammation in the substantia nigra

To further investigate whether intranasal administration of hUCMSC-Exos could improve the motor function of MPTP-induced PD mice by rescuing dopaminergic neurons, we labeled dopaminergic neurons with TH, and observed the changes in the number of dopaminergic neurons in the SNpc of mice. Cell body and protrusions of normal mouse dopaminergic neurons were distinctly immunopositive. The number of TH-positive cells and fibers in the SNpc of MPTP-treated mice was significantly reduced until day 21, and the number of TH-positive cells in the MPTP + PBS group was still maintained at a low level. However, the number of TH-positive cells in the MPTP + Exo group was significantly higher than that in the MPTP + PBS group on day 18 and remained at a high level until day 21 (Fig. 5(**A-C**)). This result suggests that intranasal administration of hUCMSC-Exos has a good neuroprotective effect in PD mouse models by rescuing the death of dopaminergic neurons in the SNpc region.

Similarly, to determine whether exosomes could modulate the activation and inflammatory response of microglia and astrocytes in the SNpc region, we assessed glial cell activation by immunostaining for IBA1 and GFAP. As shown in Fig. 6, $IBA1^{+}$ and $GFAP^{+}$ signals were significantly enhanced and the cells became swollen after MPTP treatment, indicating that both microglia and astrocytes in the SNpc region were activated. Compared with normal mice, $IBA1^{+}$ and $GFAP^{+}$ cells infiltrated into the SNpc region after MPTP treatment. However, after treatment, the number of microglia and astrocytes in the SNpc region was significantly reduced in the MPTP + Exo group compared with the MPTP + PBS group, and their morphology returned to normal by day 21, indicating a decrease in inflammation in this region (Fig. 6(**A-G**)).

Proliferation signaling assays was also performed at the corresponding time points, and no significant cell proliferation in the SNpc was observed in all groups (Fig. S3(**A**)). In addition, we also detected changes in phosphorylated α-syn level, but no obvious positive signal was observed, which may be due to the limitation of this model (Fig. S3(**B**)). All these results suggest that intranasal administration of hUCMSC-Exos not only protects against MPTP-induced death of

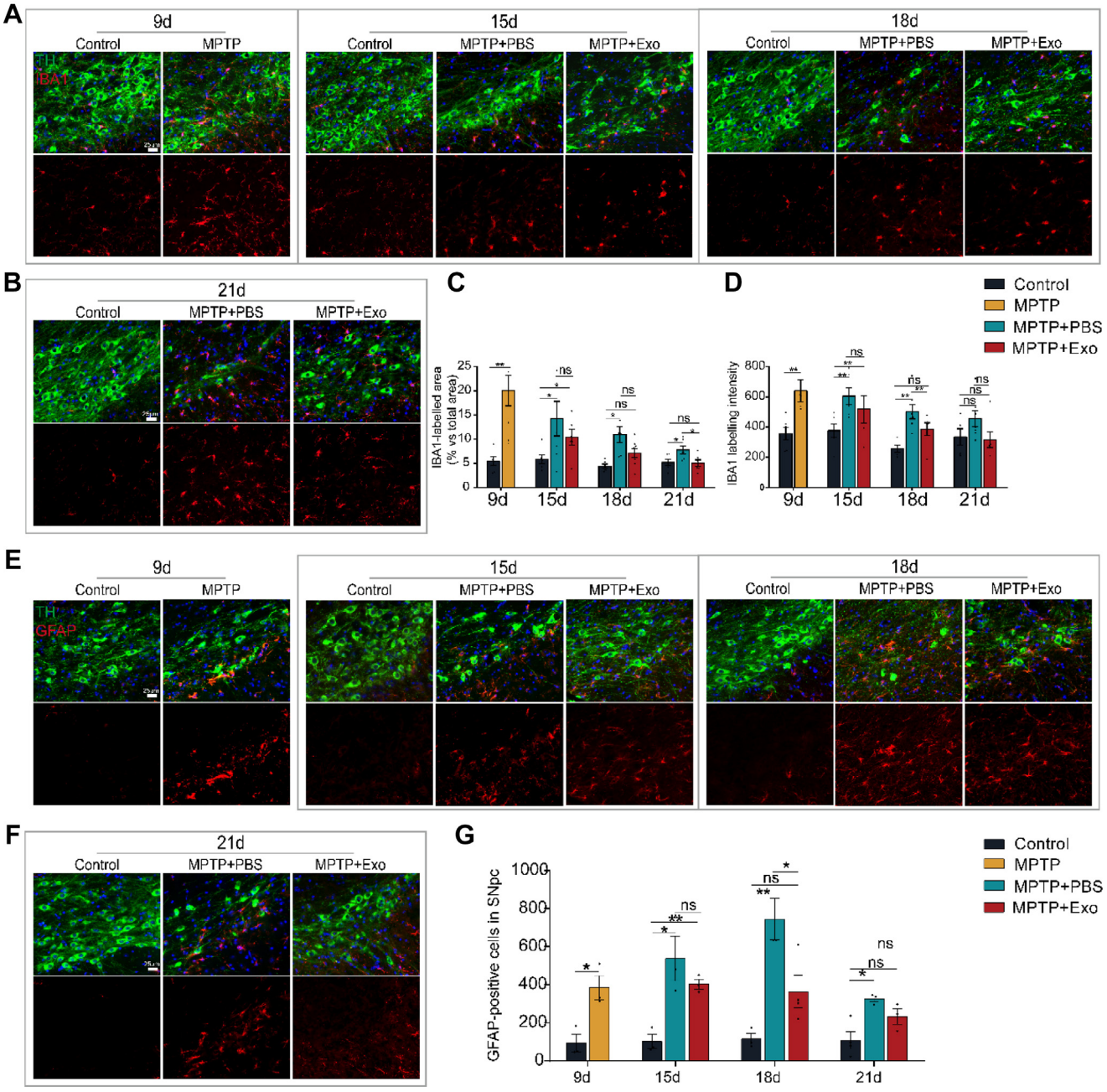

Fig. 6. Changes in microglia and astrocytes in the substantia nigra pars compacta (SNpc) of mice during intranasal administration of human umbilical cord mesenchymal stem cell-derived exosomes (hUCMSC-Exos). (**A-B**) Changes in microglia in the SNpc at different treatment time points. IBA1 (red) labels microglia, tyrosine hydroxylase (green) labels dopaminergic neurons, and Hoechst33342 (blue) labels the nuclei. Scale bar = 25 μm. (**C-D**) The immunolabelling area (C) and intensity (D) of IBA1-positive cells in the SNpc. The horizontal coordinate is the treatment time, the vertical coordinate is the area or the intensity of IBA1-positive cells, and different colors represent different treatments. $n = 6$, data are expressed as mean ± SEM and were analyzed using one-way analysis of variance. $^{*}P < 0.1$, $^{**}P < 0.01$, $^{***}P < 0.001$, ns means no significance. (**E-F**) Changes in astrocytes in the SNpc at different treatment time points. GFAP (red) labels microglia, tyrosine hydroxylase (green) labels dopaminergic neurons and Hoechst33342 (blue) labels the nuclei. Scale bar = 25 μm. (**G**) Counts of astrocytes in the SNpc. The horizontal coordinate is the treatment time, the vertical coordinate is the number of GFAP-positive cells, and different colors represent different treatments. $n = 3$, data are expressed as mean ± SEM and were analyzed using one-way analysis of variance. $^{*}P < 0.1$, $^{**}P < 0.01$, $^{***}P < 0.001$, ns means no significance. (For interpretation of the references to colour in this figure legend, the reader is referred to the web version of this article.)

dopaminergic neurons, but also attenuates MPTP-induced activation of microglia and astrocytes in the SNpc (Fig. 7).

Discussion

In recent years, exosomes have been recognized as powerful vehicles for intercellular communication, but have different biological activities due to different cell origins (Hade et al., 2021). Herein, we selected hUCMSC-Exos, because hUCMSCs have a higher proliferative capacity and faster self-renewal rate (Hsieh et al., 2010). hUCMSC-Exos have been reported to be anti-inflammatory (Thomi et al., 2019). Exosomes have been applied to a variety of neurological diseases, such as Alzheimer's disease and traumatic brain injury (Zhai et al., 2021; Zhu et al., 2022). Therefore, we envisioned that

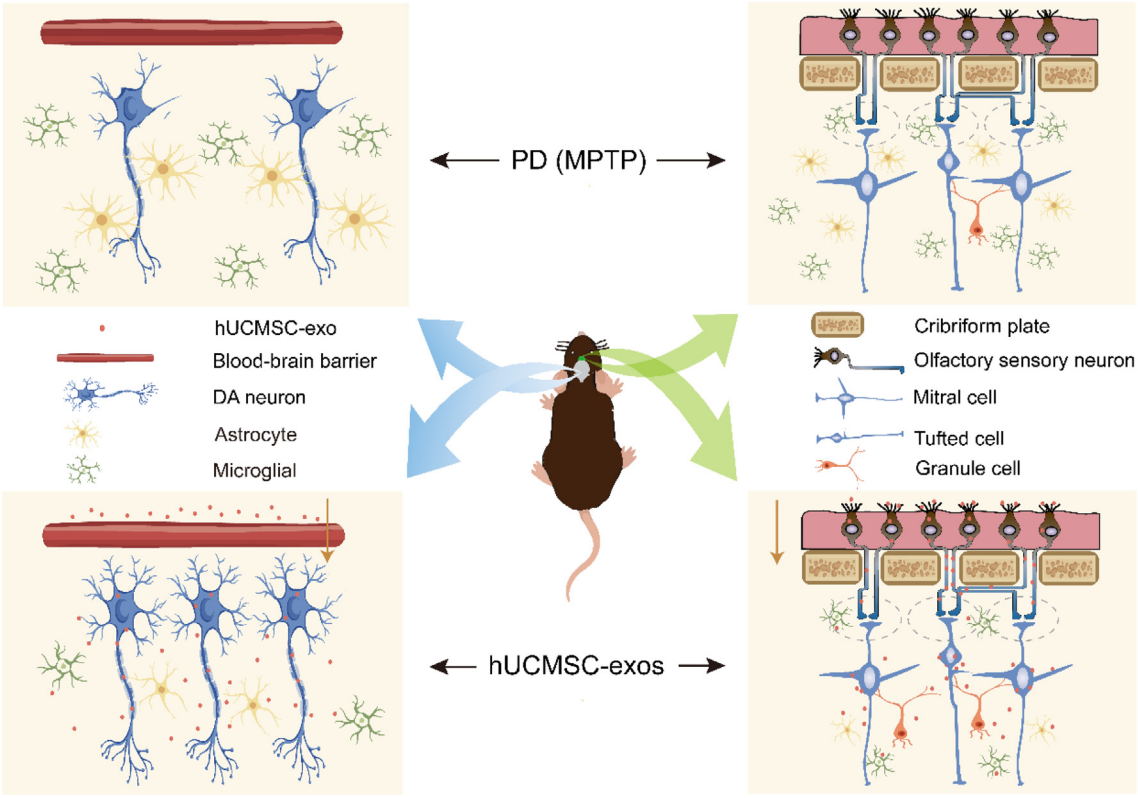

Fig. 7. Schematic diagram of exosome delivery and potential therapeutic mechanisms.

hUCMSC-Exos could be used to treat PD. In the present study, hUCMSC-Exos were actively endocytosed by astrocytes, microglia, and olfactory bulb neurons *in vitro*. After further intranasal administration of hUCMSC-Exos, it was found that exosomes had an obvious orbit around the nuclei in the mitral cell layer layer of the olfactory bulb and SNpc region. Therefore, hUCMSC-Exos could cross the blood–brain barrier and exhibit active migration to the lesion site. However, we found a small number of aggregated exosomes near the hippocampus in mice, and the rest regions of the brain were also diffusely distributed with exosomes, suggesting that the targeting of exosomes is not precise enough. Recently, engineered exosomes as a nano-delivery system have occupied an important position in regenerative medicine (Herrmann et al., 2021). What is noteworthy is that to improve the targeting of exosomes, some researchers have modified exosomes to target specific cells or regions (Peng et al., 2022; Wang et al., 2022). Therefore, whether hUCMSC-Exos can be modified to specifically target the olfactory bulb and midbrain region while ensuring their activity and integrity may be our next goal.

MPTP-induced PD mice can develop typical non-motor symptoms such as olfactory dysfunction. This dysfunction is present in about 90% of clinical early PD cases and can precede motor symptoms by several years (Doty, 2012). It has been demonstrated that non-demented subjects with PD may be at a higher risk of developing dementia 2–6 years after a decline in olfactory performance and that olfactory dysfunction is not affected by dopamine replacement medications (Bohnen et al., 2010). However, the mechanism of olfactory dysfunction is currently unknown and there are no effective means of prevention and treatment. In this study, intranasal administration of hUCMSC-Exos could significantly improve the olfactory function of PD mice, and the exosome treatment increased the activity of olfactory bulb cells and decreased the activation of glial cells in the olfactory bulb, which together promoted the recovery of olfaction in PD mice. In addition, intranasal administration is a noninvasive method, which can transport drugs directly from the nose to the brain (Zhuang et al., 2011). This implies that this novel exosome delivery method has great application value in both early clinical prevention and treatment of PD.

The MPTP-induced PD mouse model also has an advantage that it can produce pathological manifestations similar to those of human PD, including progressive degeneration and death of dopaminergic neurons in the SNpc and the appearance of characteristic motor dysfunction (Schober, 2004). Current clinical treatments for PD can only provide short-term improvements in behavioral performance and cannot rescue dopaminergic neurons from death. In the present study, we found that hUCMSC-Exos treatment greatly improved the locomotor ability of PD model mice and significantly increased the number of dopaminergic neurons in the SNpc region, suggesting that hUCMSC-Exos can rescue the death of dopaminergic neurons in the substantia nigra. In addition, it has been suggested that early astrocyte dysfunction may trigger recruitment of phagocytic microglia that subsequently target specific neurons in distinct brain regions to induce the clinical PD manifestations (Halliday and Stevens, 2011). Consequently, intercellular crosstalk between glial cells and neurons facilitates the development of PD in a neuroinflammatory milieu (Wang et al., 2023). In the present study, treatment with hUCMSC-Exos progressively normalized the morphology of dopaminergic neurons and two types of glial cells in the SNpc region. Subsequently, cell activation decreased, and inflammation and local microenvironment were improved, resulting in a gradual return of neurons and glial cells to a mutually supportive state. These cascade reactions triggered the improvement in pathological symptoms of mice with PD. Nevertheless, further investigation is needed to identify the specific intercellular communication and cytokines involved.

Neurogenesis in the adult brain is primarily limited to two distinct regions: the subventricular zone and the subgranular zone of the dentate gyrus (Doetsch and Alvarez-Buylla, 1996; Garcia-Verdugo et al.,

1998). Newly generated neural progenitor cells in the subventricular zone migrate along the rostral migratory stream into the olfactory bulb and then differentiate into granule cells and interneurons (Gould and Gross, 2002). Treatment with MPTP has been proved to decrease the number of proliferating and differentiated cells in the olfactory bulb. Furthermore, the number of neural progenitor cells in the subventricular zone begins to increase at about 3 weeks after neurogenesis is damaged, suggesting that MPTP damage leads to the activation of self-repair processes (He and Nakayama, 2015). In the present study, we compared the results of Edu on days 15 and 18 and found a significant reduction in the number of proliferating cells in the MPTP + PBS group compared with the control group on day 18. However, the number of proliferating cells increased significantly on day 18 after intranasal administration of hUCMSC-Exos, indicating that exosomes promoted the self-repair process. This may be another key factor for exosomes to promote olfactory recovery in PD mice.

In conclusion, our study demonstrates that administered intranasally hUCMSC-Exos can cross the blood–brain barrier, increase neuronal activity in the olfactory bulb of PD mice and promote self-repair mechanisms. This method can save dopaminergic neurons from death, reduce glial activation in the olfactory bulb and substantia nigra region, decrease inflammatory responses, and improve the local microenvironment in PD mice. All these findings support the restoration of olfactory and motor functions in mice with MPTP-induced PD. The intranasal administration of hUCMSC-Exos may be a promising strategy for the clinical prevention and early treatment of PD.

Ethics Statement

All animal protocols were approved by the Committee of Nantong University and the Administration Committee of Experimental Animals, Jiangsu Province, China (Approval ID: SYXK [SU] 2017–0046).

Funding

This work was supported by the National Natural Science Foundation of China (grant numbers No. 32130060 and No. 82301564); and the Natural Science Foundation of Jiangsu Province (grant numbers No. BK20202013).

Disclosure statement

The authors declare no competing interests.

CRediT authorship contribution statement

Weixiao Huang: Data curation, Formal analysis, Methodology, Project administration. **Tao Zhang:** Data curation, Formal analysis. **Xiaodi Li:** Data curation, Methodology, Validation. **Leilei Gong:** Data curation, Methodology, Project administration, Supervision. **Yu Zhang:** Data curation, Formal analysis. **Chengcheng Luan:** Methodology, Software. **Qi Shan:** Methodology, Software. **Xiaosong Gu:** Funding acquisition, Supervision, Writing – review & editing. **Lili Zhao:** Data curation, Funding acquisition, Writing – original draft.

Appendix A. Supplementary data

Supplementary data to this article can be found online at https://doi.org/10.1016/j.neuroscience.2024.04.010.

References

Bohnen, N.I., Muller, M.L.T.M., Kotagal, V., Koeppe, R.A., Kilbourn, M.A., Albin, R.L., Frey, K.A., 2010. Olfactory dysfunction, central cholinergic integrity and cognitive impairment in Parkinson's disease. Brain 133, 1747–1754.
Braak, H., Del Tredici, K., 2017. Neuropathological staging of brain pathology in sporadic Parkinson's disease: separating the wheat from the chaff. J. Parkinsons Dis. 7, S71–S85.
Brill, M.S., Ninkovic, J., Winpenny, E., Hodge, R.D., Ozen, I., Yang, R., Lepier, A., Gascon, S., et al, 2009. Adult generation of glutamatergic olfactory bulb interneurons. Nat Neurosci 12, 1524–1533.
Cai, Y., Zhang, M.M., Wang, M., Jiang, Z.H., Tan, Z.G., 2022. Bone marrow-derived mesenchymal stem cell-derived exosomes containing Gli1 alleviate microglial activation and neuronal apoptosis in vitro and in a mouse Parkinson disease model by direct inhibition of Sp1 signaling. J. Neuropathol. Exp. Neurol. 81, 522–534.
Chia, S.J., Tan, E.K., Chao, Y.X., 2020. Historical perspective: models of Parkinson's disease. Int. J. Mol. Sci. 21.
Doetsch, F., Alvarez-Buylla, A., 1996. Network of tangential pathways for neuronal migration in adult mammalian brain. Proc. Natl. Acad. Sci. U.S.A. 93, 14895–14900.
Doty, R.L., 2012. Olfactory dysfunction in Parkinson disease. Nat. Rev. Neurol. 8, 329–339.
Elsharkasy, O.M., Nordin, J.Z., Hagey, D.W., de Jong, O.G., Schiffelers, R.M., Andaloussi, S.E., Vader, P., 2020. Extracellular vesicles as drug delivery systems: why and how? Adv. Drug. Deliv. Rev. 159, 332–343.
Fullard, M.E., Morley, J.F., Duda, J.E., 2017. Olfactory dysfunction as an early biomarker in Parkinson's disease. Neurosci. Bull. 33, 515–525.
Gao, A., McCoy, H.M., Zaman, V., Shields, D.C., Banik, N.L., Haque, A., 2022. Calpain activation and progression of inflammatory cycles in Parkinson's disease. Front. Biosci. (Landmark Ed.) 27, 20.
Garcia-Verdugo, J.M., Doetsch, F., Wichterle, H., Lim, D.A., Alvarez-Buylla, A., 1998. Architecture and cell types of the adult subventricular zone: in search of the stem cells. J. Neurobiol. 36, 234–248.
Gould, E., Gross, C.G., 2002. Neurogenesis in adult mammals: some progress and problems. J. Neurosci. 22, 619–623.
Hade, M.D., Suire, C.N., Suo, Z., 2021. Mesenchymal stem cell-derived exosomes: applications in regenerative medicine. Cells 10.
Halliday, G.M., Stevens, C.H., 2011. Glia: initiators and progressors of pathology in Parkinson's disease. Mov. Disord. 26, 6–17.
He, X.J., Nakayama, H., 2015. Transiently impaired neurogenesis in MPTP mouse model of Parkinson's disease. Neurotoxicology 50, 46–55.
Herrmann, I.K., Wood, M.J.A., Fuhrmann, G., 2021. Extracellular vesicles as a next-generation drug delivery platform. Nat. Nanotechnol. 16, 748–759.
Hong, D.G., Lee, S., Kim, J., Yang, S., Lee, M., Ahn, J., Lee, H., Chang, S.C., et al, 2022. Anti-inflammatory and neuroprotective effects of morin in an MPTP-induced Parkinson's disease model. Int. J. Mol. Sci. 23.
Hsieh, J.Y., Fu, Y.S., Chang, S.J., Tsuang, Y.H., Wang, H.W., 2010. Functional module analysis reveals differential osteogenic and stemness potentials in human mesenchymal stem cells from bone marrow and Wharton's jelly of umbilical cord. Stem Cells Dev. 19, 1895–1910.
Jankovic, J., Tan, E.K., 2020. Parkinson's disease: etiopathogenesis and treatment. J. Neurol. Neurosurg. Psychiatry 91, 795–808.
Kalia, L.V., Lang, A.E., 2015. Parkinson's disease. Lancet 386, 896–912.
Kalluri, R., LeBleu, V.S., 2020. The biology, function, and biomedical applications of exosomes. Science 367.
LaFever, B.J., Kawasawa, Y.I., Ito, A., Imamura, F., 2022. Pathological consequences of chronic olfactory inflammation on neurite morphology of olfactory bulb projection neurons. Brain Behav. Immun. Health 21, 100451.
Langston, J.W., Ballard, P., Tetrud, J.W., Irwin, I., 1983. Chronic Parkinsonism in humans due to a product of meperidine-analog synthesis. Science 219, 979–980.
Latif, S., Jahangeer, M., Maknoon Razia, D., Ashiq, M., Ghaffar, A., Akram, M., El Allam, A., Bouyahya, A., et al, 2021. Dopamine in Parkinson's disease. Clin. Chim. Acta 522, 114–126.
Lei, Q., Gao, F., Liu, T., Ren, W., Chen, L., Cao, Y., Chen, W., Guo, S., et al, 2021. Extracellular vesicles deposit PCNA to rejuvenate aged bone marrow-derived mesenchymal stem cells and slow age-related degeneration. Sci. Transl. Med. 13.
Losurdo, M., Pedrazzoli, M., D'Agostino, C., Elia, C.A., Massenzio, F., Lonati, E., Mauri, M., Rizzi, L., et al, 2020. Intranasal delivery of mesenchymal stem cell-derived extracellular vesicles exerts immunomodulatory and neuroprotective effects in a 3xTg model of Alzheimer's disease. Stem Cells Transl. Med. 9, 1068–1084.
Mendes-Pinheiro, B., Anjo, S.I., Manadas, B., Da Silva, J.D., Marote, A., Behie, L.A., Teixeira, F.G., Salgado, A.J., 2019. Bone marrow mesenchymal stem cells' secretome exerts neuroprotective effects in a Parkinson's disease rat model. Front. Bioeng. Biotechnol. 7, 294.
Pegtel, D.M., Gould, S.J., 2019. Exosomes. Annu. Rev. Biochem. 88, 487–514.
Peng, H., Li, Y., Ji, W., Zhao, R., Lu, Z., Shen, J., Wu, Y., Wang, J., et al, 2022. Intranasal administration of self-oriented nanocarriers based on therapeutic exosomes for synergistic treatment of Parkinson's disease. ACS Nano 16, 869–884.
Porlan, E., Perez-Villalba, A., Delgado, A.C., Ferron, S.R., 2013. Paracrine regulation of neural stem cells in the subependymal zone. Arch. Biochem. Biophys. 534, 11–19.

Schober, A., 2004. Classic toxin-induced animal models of Parkinson's disease: 6-OHDA and MPTP. Cell Tissue Res. 318, 215–224.
Song, Y., Li, Z., He, T., Qu, M., Jiang, L., Li, W., Shi, X., Pan, J., et al, 2019. M2 microglia-derived exosomes protect the mouse brain from ischemia-reperfusion injury via exosomal miR-124. Theranostics 9, 2910–2923.
Thomi, G., Surbek, D., Haesler, V., Joerger-Messerli, M., Schoeberlein, A., 2019. Exosomes derived from umbilical cord mesenchymal stem cells reduce microglia-mediated neuroinflammation in perinatal brain injury. Stem Cell Res. Ther. 10, 105.
Tolosa, E., Garrido, A., Scholz, S.W., Poewe, W., 2021. Challenges in the diagnosis of Parkinson's disease. Lancet Neurol. 20, 385–397.
Wang, Q., Li, T., Yang, J., Zhao, Z., Tan, K., Tang, S., Wan, M., Mao, C., 2022. Engineered exosomes with independent module/cascading function for therapy of Parkinson's disease by multistep targeting and multistage intervention method. Adv. Mater. 34, e2201406.
Wang, Q., Zheng, J., Pettersson, S., Reynolds, R., Tan, E.K., 2023. The link between neuroinflammation and the neurovascular unit in synucleinopathies. Sci. Adv. 9, eabq1141.
Zhai, K., Duan, H., Wang, W., Zhao, S., Khan, G.J., Wang, M., Zhang, Y., Thakur, K., et al, 2021. Ginsenoside Rg1 ameliorates blood-brain barrier disruption and traumatic brain injury via attenuating macrophages derived exosomes miR-21 release. Acta Pharm. Sin. B 11, 3493–3507.
Zhu, B., Liu, Y., Hwang, S., Archuleta, K., Huang, H., Campos, A., Murad, R., Pina-Crespo, J., et al, 2022. Trem2 deletion enhances tau dispersion and pathology through microglia exosomes. Mol. Neurodegener. 17, 58.
Zhuang, X., Xiang, X., Grizzle, W., Sun, D., Zhang, S., Axtell, R.C., Ju, S., Mu, J., et al, 2011. Treatment of brain inflammatory diseases by delivering exosome encapsulated anti-inflammatory drugs from the nasal region to the brain. Mol. Ther. 19, 1769–1779.